Draft version May 4, 2025
Typeset using LaTeX **twocolumn** style in AASTeX631

The Near-Infrared Discrete Extinction Laws of the Galactic Center

Deval Deliwala[1]

[1] *University of California, Berkeley*

ABSTRACT

The extinction law, which describes how extinction varies as a function of wavelength, is an important parameter for interpreting observations of highly reddened stellar populations. In a complex and dynamic region like the Galactic Center (GC), it is certain extinction also varies with position. We investigate a discrete and spatially varying extinction law of the GC by analyzing red clump (RC) stars across four JWST NIRCam bandpass filters – F115W, F212N, F323N, and F405N (roughly 1.15μm to 4.05μm) – in four spatial regions covering the central 120" × 120" of the GC. To enhance the accuracy of our measurements of red clump stars, we implement an iterative Markov Chain Monte Carlo (MCMC) compound Gaussian + Linear fit. We measure total extinction ratios A_λ/A_{F212N} that vary among each 60" × 60" sub field by 10% at F115W to 40% at F323N-F405N. Within uncertainties, most filter ratios agree with **?**. We detect 3σ differences only in A_{F115W}/A_{F212N} in three regions and in A_{F405N}/A_{F212N} in one. The inter-region dispersions (up to 15%) are significant at $\leq 6\sigma$ and point to genuine, sub-parsec variations in grain size and mantle composition within the Galactic Center.

1. INTRODUCTION

The interstellar extinction law is crucial for studying the structure and star formation history of the GC and other dense regions in the Milky Way. Extinction refers to the absorption and scattering of light by dust grains along the line of sight, resulting in the *reddening* of objects relative to their intrinsic magnitudes (**?**). The extinction law, which describes how this effect varies with wavelength, is essential both for correcting astronomical observations and for accurately interpreting the physical properties of stars and other objects in obscured regions. Common extinction laws like **?** and **?** describe the optical through near-infrared (OIR; 0.8μm – 2.2μm) extinction law as a single power law ($A_\lambda \propto \lambda^{-\beta}$)) with $\beta \approx 1.6$. More recent studies (e.g. **???**) show a "universal power law" of constant β is impossible.

Hence, the extinction law is not uniform throughout the galaxy; it depends on the line of sight – the physical properties of the intervening dust grains (**??**). In regions like the GC, where extreme dust obscuration occurs, determining an accurate extinction law is even more important to correct these effects and understand the underlying stellar populations (**??**).

One of the foundational methods of deriving the extinction law is the "Red Clump (RC) method," introduced by **?**. RC stars are a population of evolved stars in their core-helium burning phase. Their helium-core masses are nearly identical, and in the K-band their absolute magnitudes depend only on metallicity and age (**?**). Thus, RC stars serve as reliable infrared standard candles. Assuming a uniform intrinsic color, any color spread on a color-magnitude diagram (CMD) arises purely from interstellar extinction. Consequently, RC stars are excellent extinction probes (**??**). By analyzing the mean magnitudes and colors of red giant stars (often RC) across different wavelength bands, **??** reported steeper extinctions of $\beta = 1.9$ and 2.0 respectively towards the Galactic Bulge.

? contributed by deriving the central GC extinction law via spectroscopic observations of gas emission lines ($\lambda \geq 1\mu$m) within 20" of Sagittarius A^*. By analyzing hydrogen emission lines, an even steeper power law with $\beta = 2.11 \pm 0.06$ in this region.

? presented an updated GC extinction law in the OIR regime using Hubble Space Telescope (HST) observations of 819 RC stars. This work also found the GC extinction law to be inconsistent with a single power law and found extinction ratios at 1.25μm and 8.14μm to be 18% and 24% larger than the previously used **?** law.

Advancements in infrared astronomy and the availability of deep photometric catalogs have improved the study of extinction laws. For example, **??** conducted high-angular-resolution (∼0.2") *JHKs* imaging analysis of the GC using the GALACTICNUCLEUS survey which covers a range of ∼6kpc^2. Studies using data from the VISTA *Variables in the Via Lactea* (VVV) survey (**?**) and the Galactic Legacy Infrared Mid-Plane Survey Extraordinaire (GLIMPSE) survey (**?**) have provided extensive datasets for mapping interstellar extinc-

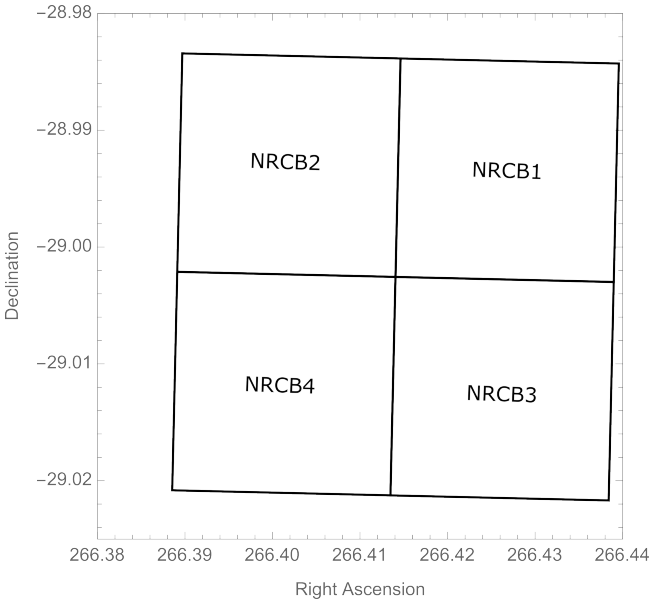

Figure 1. JWST NRCB region coverage.

tion across the Galactic plane. However, survey-based extinction studies are often dominated by low-extinction stars and are limited by the photometric depths of the survey(s). Observing RC stars compounds these challenges: extreme extinction pushes them below detection thresholds, and extreme stellar density causes source confusion. The recent release of photometric calibrated catalogs from the James Webb Space Telescope (JWST) offers an unprecedented opportunity to probe the extinction law in more detail, both in terms of wavelength coverage and possible spatial variations. JWST's superior angular resolution mitigates crowding, while its greater sensitivity reaches fainter, more heavily-reddened RC stars, enabling accurate extinction mapping in the most obscured regions.

Here, we apply the RC method to JWST NIRCam photometric catalogs. We analyze four filters – F115W, F212N, F323N, and F405N – across the near-infrared (NIR; 1.15μm-4.05μm), in four spatial regions NRCB1-4 covering the central 120" × 120" of the GC. The NRCB regions correspond to different detectors on JWST's sensor chip assembly (see Figure 1). This approach focuses on potential spatial variations and the influence of physical phenomena like ice absorption at specific wavelengths (**???**). The main goal is to determine whether significant differences in extinction exist *between* these NRCB regions and to compare our findings with the (**?**) law. This work has implications for any dense, obscured region in the Milky Way.

2. OBSERVATIONS AND MEASUREMENTS

3. METHODS

In a color-magnitude diagram (CMD) the RC cluster appears as a narrow, tilted "bar" because every star (roughly) shares the same intrinsic magnitude M_λ and color, so the *observed* shifts of those those stars are driven almost entirely by extinction. Let the two filters be λ (bluer) and λ' (redder). If we place the extinction-sensitive magnitude m_λ on the y-axis and the color $m_\lambda - m_{\lambda'}$ on the x-axis, a simple linear regression of the RC ridge gives the total-to-selective extinction ratio

$$R_\lambda = \frac{A_\lambda}{E_{\lambda'-\lambda}} = \frac{\partial m_\lambda}{\partial(m_{\lambda'} - m_\lambda)}.$$

Repeating the fit with the redder filter on the y-axis – $m_{\lambda'}$ versus the same color yields

$$R_{\lambda'} = \frac{A_{\lambda'}}{E_{\lambda'-\lambda}} = \frac{\partial m_{\lambda'}}{\partial(m_{\lambda'} - m_\lambda)}.$$

Because both regressions share the same color excess $E_{\lambda-\lambda'} = A_\lambda - A_{\lambda'}$, geometry forces the two slopes to differ by one.

$$R_{\lambda'} - R_\lambda = \frac{A_{\lambda'}}{A_{\lambda'} - A_\lambda} - \frac{A_\lambda}{A_{\lambda'} - A_\lambda} = 1.$$

Hence, measuring any single RC slope fixes the other, and their ratio yields the total extinction ratio: $R_\lambda = R_{\lambda'} - 1$. Dividing the two slopes then gives the absolute extinction ratio,

$$\frac{A_\lambda}{A_{\lambda'}} = \frac{R_\lambda}{R_{\lambda'}} = \frac{R_{\lambda'} - 1}{R_{\lambda'}},$$

so the measuring the ratio of total extinction $A_\lambda/A_{\lambda'}$ reduces to one linear regression and trivial division – a direct consequence of RC geometry in CMD space. We will derive A_λ/A_{F212N} for $\lambda \in \{\text{F115W, F323N, F405N}\}$. Thus, three slope measurements are required for every NRCB1-4 region. For simplicity, we describe the procedure for NRCB1. The same steps apply to NRCB2-4.

3.1. *Extracting the Red Clump*

First isolate the RC from the surrounding stellar population. To do this, we exploit the large extinction difference between F115W and F212N ($A_{F115WW}/A_{F212N} \approx 3.523$, **?**). This makes the RC bar steep and well-defined in the F115W - F212N vs. F115W CMD. To minimize outliers while ensuring ample RC coverage, we use the unsharp-masking technique described in **?** on these CMDs. We first convert the CMD to a Hess Diagram, which represents stellar density as a 2D histogram. Each star's position is modeled as a normal distribution, with its width determined from the associated photometric

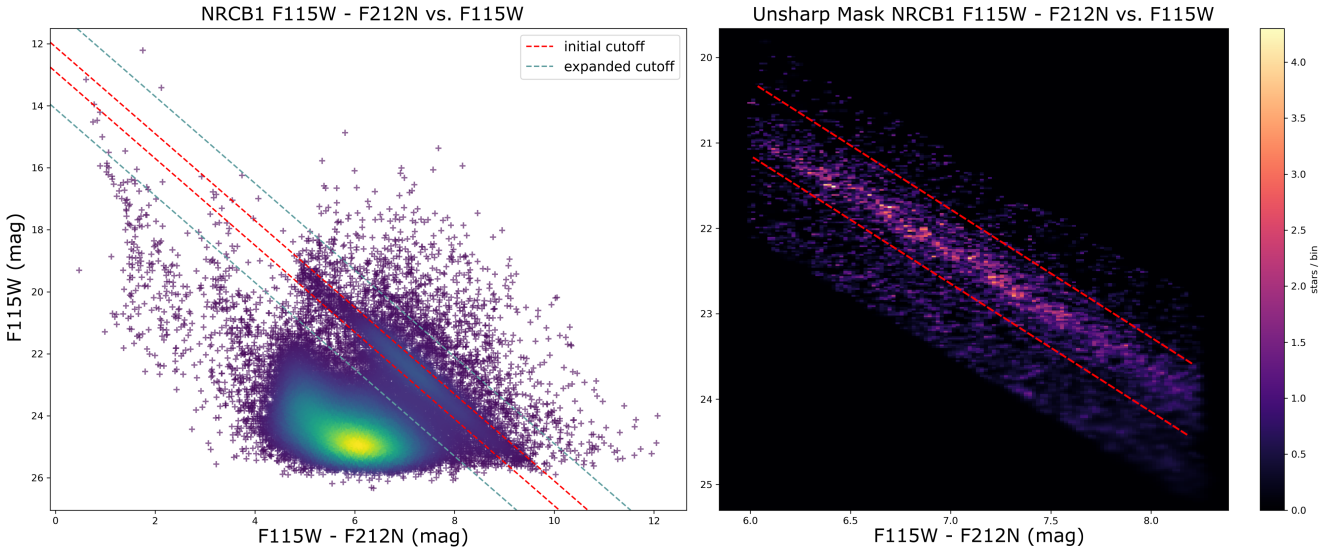

Figure 2. The selection criterion used to identify RC stars in NRCB1. Following **?** we convert the observed CMD (left panel) into a Hess diagram and apply unsharp masking to identify the high-density RC ridge. We then draw initial by-eye boundaries (red lines) around the RC feature and expand by a factor of three (aqua lines) for ample RC star coverage.

error. The histogram is built with a bin size of 0.02 mags in both color (F115W - F212N) and magnitude (F115W) space. To generate the unsharp mask, we convolve the Hess Diagram with a 2D Gaussian Kernel of 0.3 mag width. The convolved Hess Diagram is then subtracted from the original. Finally, we apply a power-law scaling with exponent $\gamma = 1.5$ via a PowerNorm transform, which enhances the contrast of the RC bar relative to the surrounding background. The resulting unsharp mask for NRCB1 F115W - F212N vs. F115W is shown on the right of Figure 2. Afterwards a tight parallel cutoff was defined by-eye that encloses the RC bar, which are expanded by a factor of three to ensure sufficient coverage. This is only a conservative ansatz, which is improved upon by the algorithm described in Section **??**.

We select the 5,027 stars in NRCB1 that lie within the expanded (aqua) boundaries and match them in the F323N and F405N catalogs. By defining the RC once in the high-contrast F115W–F212N CMD and "lifting" the selection to bluer filters, we maintain a consistent sample and avoid having to redraw the clump in each CMD, where the RC ridge is increasingly washed out.

3.2. *Curve Fitting Algorithm*

Now that we have an RC population across F115W-F405N, we fit straight lines to the RC bar in three CMDs:

- F115W - F212N vs. F115W
- F212N - F323N vs. F323N
- F212N - F405N vs. F212N

We chose each magnitude-color pairing based on the RC's contrast after unsharp masking the RC population, but the exact choice is not critical: as shown in Section 1, measuring the slope in one projection fixes the slope in the complementary CMD by a difference of one.

There are **two types of CMDs**: ones that have a prominent RC bar and ones that do not. F115W - F212N vs. F115W and F212N - F405N vs. F212N fall into category one, with crisp, high-contrast RC bars, whereas F212N - F323N vs. F323N falls into category two. This makes sense: 2.12μm and 3.23μm are close in wavelength so their extinctions are similar, and uneven ice absorption features around 3μm further blur the clump feature (**?**). Therefore, we implement two methods of measuring the RC bar slope.

1. **Compound Gaussian + Linear MCMC fits.** Models the RC ridge as multiple Gaussian+Linear distributions, then uses MCMC to jointly fit both components, yielding a robust slope estimate when the clump is well defined. (F115W - F212N vs. F115W and F212N - F405N vs. F212N)

2. **Linear MCMC fit with Monte Carlo jitter.** Fits a simple linear model via MCMC and assesses its variance via Monte Carlo perturbing the initial CMD selection boundaries 500 times. Although less statistically powerful, this jitter approach is essential for CMDs where resolution is lacking and/or the RC bar is washed out, as it isolates sensitivity to boundary choice. (F212N - F323N vs. F323N)

3.3. *Type 1*

1. Divide RC range into n tiles.
2. For each tile k = 1..n:
   a. Select stars in tile k.
   b. Fit Gaussian + Linear MCMC.
   c. Record mean magnitude μ_k.
3. Collect points (tile_center$_k$, μ_k) $\forall k$
4. Fit Linear μ = m(tile_centers) + b.
5. Return slope m.

Roughly, the procedure begins by dividing the RC bar into $n = 10$ contiguous tiles. Within each tile we fit a compound Gaussian + Linear model using MCMC. The Gaussian component captures the RC overdensity while the linear component describes the background trend. After extracting the mean magnitude from each Gaussian fit, we perform a simple linear regression through those $n = 10$ mean points to determine the overall RC slope.

However, the tiles have to lay *along* the RC ridge to produce MCMC means that follow the ridge itself. To accomplish this, we first rotate the CMD by $\theta = \tan^{-1}(m_{\rm ansatz})$ where $m_{\rm ansatz}$ is the slope of the provisional parallel cutoffs defined in Section 3.1. This rotation renders the RC bar (roughly) horizontal. We then lay down n vertical, contiguous tiles across the full length of the horizontal bar, and finally rotate the tiles *back* to the original CMD frame. In this frame the tiles are now orthogonal to the RC ridge, ensuring that the mean magnitude extracted from each tile follows the ridge. This process is visualized in Figure 3. A choice of $n = 10$ was made and justified in Section **??**.

3.3.1. *Rotation*

Now the stars in each tile are extracted, and put through the MCMC fit. However, the tiles cut across the CMD at an angle that follows the RC ridge. Fitting the y magnitude 1-D distribution would therefore mix intrinsic RC width with the geometric tilt of the tile. Consequently for every tile we apply the counterclockwise rotation

$$\begin{pmatrix} x_{\rm rot} \\ y_{\rm rot} \end{pmatrix} = \begin{pmatrix} \cos\theta & -\sin\theta \\ \sin\theta & \cos\theta \end{pmatrix} \begin{pmatrix} x \\ y \end{pmatrix} = \vec{R} \begin{pmatrix} x \\ y \end{pmatrix}$$

where $\theta = \tan^{-1}\big(m_{\rm ansatz}\big)$.

Now, the 1-D distribution of $y_{\rm rot}$ inside each tile can be treated as a sum of a narrow Gaussian bump (RC stars) and a gentle varying continuum (everything else). Only $y_{\rm rot}$ enters the likelihood; $x_{\rm rot}$ is used later to place the representative mean point back on the CMD.

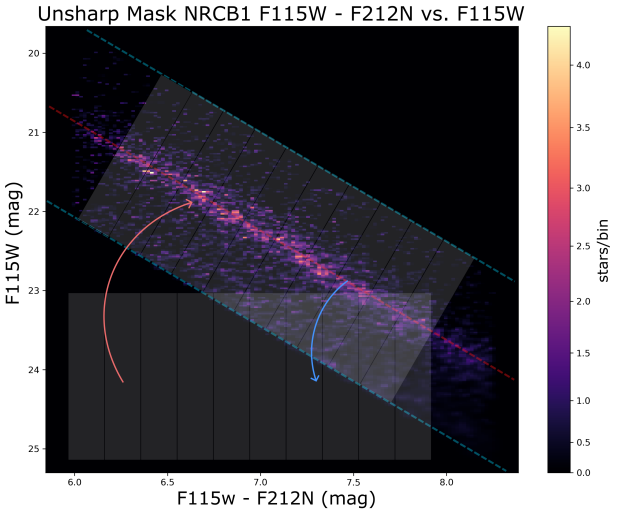

Figure 3. Generating tiles that run *along* the RC bar to guide the collective MCMC slope fit. First, we rotate the CMD by an angle $\theta = \tan^{-1}(m_{\rm ansatz})$ so that the RC ridge becomes horizontal. We then place $n = 10$ vertical bins across this rotated RC, and rotate the bins back into the original CMD basis, now orthogonal to the ansatz RC slope.

3.3.2. *Mixture Model*

For a single histogram bin center y_i (after rotation), with observed count n_i and Poisson error $\sigma_i = \sqrt{n_i + 1}$, we posit the intensity model

$$\lambda(y_i|\vec{\theta}) = A \exp\left[-\frac{1}{2}\left(\frac{y_i - \mu}{\sigma}\right)^2\right] + (1 - f_{\rm RC})(m y_i + b)$$

with parameter vector

$$\vec{\theta} = (u, A, \mu, \sigma, m, b), \quad f_{\rm RC} = \frac{1}{1 + e^{-u}} \in (0, 1).$$

where

- A, μ, σ describe the Gaussian-component RC peak.
- m, b describe the Linear-component non-RC continuum.
- $f_{\rm RC}$ is the *fraction* of all stars in the tile that belong to the RC component. We sample its logit $u \in \mathbb{R}$, rather than $f_{\rm RC}$ itself, so that walker diffusion is unrestricted, instead of sampling a fraction in $[0, 1]$. This also reduces the integrated autocorrelation time as described in Section **??**.

Assuming independent Gaussian noise, the log-likelihood for one tile is

$$\ln \mathcal{L} = -\frac{1}{2} \sum_i \Big[n_i - \lambda(y_i|\vec{\theta})\Big]^2 / \sigma_i^2 - \frac{1}{2} \sum_i \ln(2\pi\sigma_i^2).$$

3.3.3. *Priors*

We impose weakly informative but physically motivated priors

$$\begin{aligned} u &\sim \text{logit-Beta}(\alpha = 3, \beta = 2), \\ A &\sim \mathcal{U}(0, 10^3), \\ \mu &\sim \mathcal{U}(\bar{y} - 2s, \bar{y} + 2s), \\ \sigma &\sim \mathcal{U}(\max\{0, s - 0.5\}, s + 0.5), \\ m &\sim \mathcal{U}(-\infty, 30), \quad b \sim \mathcal{U}(-\infty, 50), \end{aligned}$$

where $\bar{y}$ and s are the sample mean and standard deviation of $y_{\rm rot}$. Priors are zero outside the stated intervals, so the overall log-prior is $-\infty$ whenever a walker steps outside these bounds. Values $\alpha = 3, \beta = 2$ reflects our expectation that – within a well-selected tile – a majority of stars may be RC. However, the prior remains fairly broad ($\text{Var}[\text{Beta}(3, 2)] = 0.04$), letting the data dominate whenever there are enough counts. After sampling in the unbounded logit variable u, we include the Jacobian $\ln[f(1 - f)]$ to correctly map back to a $\text{Beta}(\alpha, \beta)$ prior on $f_{\rm RC}$.

3.3.4. *Posterior Sampling*

The posterior

$$\ln p(\vec{\theta} \mid \text{data}) = \ln \mathcal{L} + \ln p(\vec{\theta})$$

is mapped with an affine-invariant `EnsembleSampler` from **emcee** (**?**). The sampler is set for 64 walkers, 15000 steps, with a 1000 step burn-in. These values are justified from the autocorrelation analysis described in Section **??**. For every tile we store

$$\langle\mu\rangle, \langle\sigma\rangle, \langle A\rangle, \langle f_{\rm RC}\rangle,$$

as the posterior medians, and the posterior standard deviation of μ,

$$\sigma_\mu = \sqrt{\text{Var}_{\rm post}(\mu)},$$

serves as the uncertainty on the RC centroid (still in the rotated basis).

3.3.5. *Back-rotation*

The representative CMD position (original basis) of the tile is

$$\vec{r}_{\rm CMD} = \vec{R}^T \begin{pmatrix} \langle x_{\rm rot}\rangle \\ \langle\mu\rangle \end{pmatrix}$$

where $\langle x_{\rm rot}\rangle$ is the median $x_{\rm rot}$ of all the stars in the tile. Uncertainty propagation (back to CMD frame) uses

$$\vec{\sigma}_{\rm CMD} = \vec{R}^T \begin{pmatrix} 0 \\ \sigma_\mu \end{pmatrix}, \qquad \sigma_y = |(\vec{\sigma}_{\rm CMD})_2|.$$

Only tiles with $\sigma_y \leq 0.3$ mag, $f_{\rm RC} > 0.01$ (insignificant RC population), and have satisfied autocorrelation as described in Section **??** are retained for the final linear regression.

3.3.6. *Weighted slope of the RC bar*

The total RC *area* inside each tile is

$$\mathcal{A}_i = A_i \sigma_i \sqrt{2\pi}, \quad A_i^{(\rm norm)} = \frac{\mathcal{A}_i}{\max_j \mathcal{A}_j} \in (0, 1].$$

Adopting the inverse-variance logic of χ^2 fitting, but down-weighting tiles where the RC population is intrinsically faint or poorly populated (smaller $f_{\rm RC}$), we assign

$$w_i = A_i^{(\rm norm)} \frac{f_{\rm RC,i}}{\sigma_{y,i}^2}.$$

Finally, a weighted linear regression through the representative points from all tiles $(x_i, y_i) = (\vec{r}_{\rm CMD})^T$ yields

$$y = \hat{m}x + \hat{b}, \quad \text{Cov}(\hat{m}, \hat{b}) = C, \quad \sigma_{\hat{m}} = \sqrt{C_{00}}.$$

The pair $(\hat{m} \pm \sigma_{\hat{m}})$ constitutes the final extinction ratio. This procedure is performed for F115W - F212N vs. F115W and F212N - F405N vs. F405N in every NRCB1-4.

4. TYPE 2

1. Pick two guide points + gap g.
2. Anchor line $y = m_0 x + b_0$.
3. Select stars $|y - (m_0 x + b_0)| \leq g$.
4. Keep densest $f_{\rm top}$ fraction via KDE.
5. Fit Bayesian line (MCMC).
   a. Returns slope $m \pm \sigma_{\rm stat}$.
5. Jitter slopes ($\pm 10\%$, $N = 500$ trials).
   b. Returns $\sigma_{\rm sys}$.
6. Return slope $m \pm \sqrt{\sigma_{\rm stat}^2 + \sigma_{\rm sys}^2}$.

From the JWST photometric catalogs we work with the color

$$x = m_{F212N} - m_{F323N}$$

and magnitude

$$y = m_{F323N}, \quad \sigma_y = \text{photometric } 1 - \sigma \text{ error}.$$

Two bye-eye points (x_1, y_1) and (x_2, y_2) plus a half-width gap g specify an initial strip

$$\mathcal{B}_0 = \left\{(x, y) : \Big| \, y - (m_0 x + b_0) \Big| \leq g \right\},$$

where

$$m_0 = \frac{y_2 - y_1}{x_2 - x_1}, \; b_0 = y_1 - m_0 x_1.$$

To avoid diluting the fit with sparse outskirts, we retain only the densest $f_{\rm top}$ of points inside $\mathcal{B}_0$. Density is estimated via a 2D kernel density estimator (KDE),

$$\rho(x, y) = \hat{p}_{\rm KDE}(x, y),$$

and we keep those stars whose ρ exceeds the (1-$f_{\rm top}$)-quantile of the KDE distribution. In practice we set $f_{\rm top} = 0.4$ to give an ample number of stars for a robust fit while focusing on the RC. This process is visualized in Figure 4.

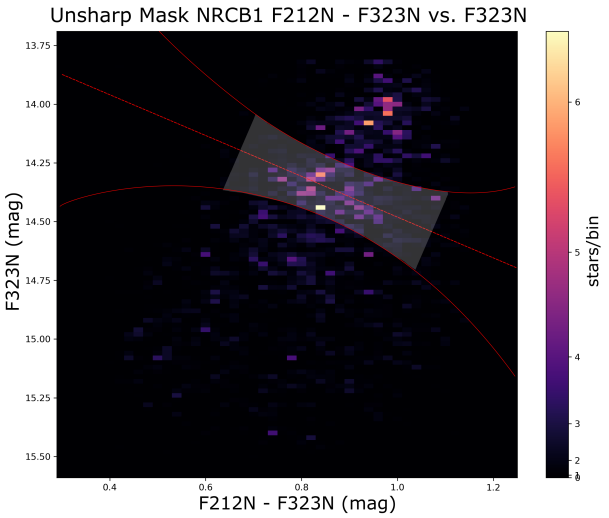

Figure 4. RC-bar slope calculation in F212N - F323N vs. F323N CMD. The by-eye ansatz slope is shown in red and its shaded ± gap g band shows both the initial selection strip and the range over which we apply ±10% slope jitter when estimating systematic uncertainty.

4.0.1. *Bayesian model*

Let the final filtered set contain N stars. We posit the data-generating equation

$$y_i = mx_i + b + \varepsilon_i, \quad \varepsilon_i \sim \mathcal{N}(0, \sigma_y^2(x_i) + \sigma_{\rm int}^2),$$

where

- m, b are the RC slope and intercept.
- $\sigma_y(x_i)$ is the known photometric error.
- $\sigma_{\rm int}$ is any other error besides measurement.

Sampling in logarithmic space, $\log \sigma_{\rm int} \equiv \eta$, keeps the parameter unbounded. The log-likelihood is

$$\ln \mathcal{L}(m, b, \eta) = -\frac{1}{2} \sum_{i=1}^{N} \left[\frac{(y_i - (mx_i + b))^2}{\sigma_y^2(x_i) + e^{2\eta}} + \ln(2\pi \left[\sigma_y^2(x_i) + e^{2\eta}\right]) \right].$$

We adopt broad priors

$$m \sim \text{Uniform}(-10^3, 10^3), \quad b \sim \text{Uniform}(-10^6, 10^6),$$

and

$$p(\eta) \propto \exp\left(-\frac{1}{2}\eta^2\right),$$

The posterior is explored with 40 affine-invariant walkers for 6000 steps with a 1000 step burn-in. We define the posterior medians $\hat{m}, \hat{b}, \hat{\sigma_{\rm int}}$ and the statistical $1-\sigma$ error,

$$\sigma_{\hat{m},\rm stat} = \sqrt{\text{Var}_{\rm post}(m)}.$$

4.1. *Systematics via Monte Carlo jitter*

To gauge "how much the result depends on the initial by-eye strip", we run $N_{\rm jit}$ random "jitter" experiments:

1. Multiply the provisional slope m_0 by $1 + \delta$ with $\delta \sim \mathcal{N}(0, 0.10^2)$ (±10%) scatter.
2. Re-anchor the line so it passes through the midpoint $\left(\frac{1}{2}(x_1 + x_2), \frac{1}{2}(y_1 + y_2)\right)$.
3. Re-select stars within the same gap g, fit a weighted lease-squares slope $m_{\rm jit}^{(k)}$.

If at least two jitters succeed, their sample standard deviation

$$\sigma_{\hat{m},\rm sys} = \sqrt{\frac{1}{N_{\rm jit} - 1} \sum_k \left(m_{\rm jit}^{(k)} - \bar{m}_{\rm jit}\right)^2}$$

is taken as the systematic uncertainty due to the initial ansatz strip. The final slope measurement is therefore

$$\hat{m} \pm \sigma_{\hat{m}}, \quad \sigma_{\hat{m}} = \sqrt{\sigma_{\hat{m},\rm stat}^2 + \sigma_{\hat{m},\rm sys}^2}.$$

This method is only used for F212N - F323N vs. F323N CMDs across NRCB1-4, when the RC bar is not as well-defined.